UNCLASSIFIED

AD **274 032**

Reproduced
by the

ARMED SERVICES TECHNICAL INFORMATION AGENCY
ARLINGTON HALL STATION
ARLINGTON 12, VIRGINIA

UNCLASSIFIED

274 032

FINAL REPORT ON THE THEORY
AND OPERATION OF A FIVE-FOOT-DIAMETER BETATRON
WITH EXTERNAL INJECTION

D.C. de Packh

Nuclear Interactions Branch
Nucleonics Division

March 27, 1962

U. S. NAVAL RESEARCH LABORATORY
Washington, D.C.

CONTENTS

ABSTRACT

A five-foot-diameter experimental betatron with a beam-containing tube approximately one inch in cross-sectional diameter and having alternating air-core quadrupole focusing and an external injection system has been built and successfully tested. The behavior of the injected electrons was found to be in reasonable agreement with theory. These results indicate the direction to be taken in future experiment of a similar nature.

PROBLEM STATUS

This is a final report on the problem, which was closed on June 30, 1960.

AUTHORIZATION

FINAL REPORT ON THE THEORY AND OPERATION OF A
FIVE-FOOT-DIAMETER BETATRON WITH EXTERNAL INJECTION

SCOPE OF THE PROBLEM AND SUMMARY OF RESULTS

This project originally had in view the development of an ironless synchrotron with solenoid focusing. It is not the purpose of the present report to go into the details of this early work, but rather to describe the more recent efforts aimed at radical departures in accelerator design. It is nevertheless useful for reasons of orientation to devote a few sentences to the historical aspect. The basic concept of the older solenoid-focused machine was that of a variable operating point. (The operating point is defined in accelerator theory as a pair of values, one for each of the two principal transverse directions, of the ratio of machine radius to betatron radian length, or "mode number.") It was realized that an operating point which varies adiabatically gives rise to catastrophic particle losses when the mode number is an integer or half-integer. It was hoped, nevertheless, that programming the solenoid current so that these resonant regions could be traversed quickly would make these losses innocuous. For a variety of reasons this hope turned out to be ill-founded, and it was decided to abandon the variable operating point design for one using a fixed operating point. This could not be done with solenoid lenses in the available space since the implied power dissipation in the lenses is excessive. For this reason a quadrupole-focused system was chosen for the new design (1).

Advances in design of other forms of particle accelerator, particularly the linac, had in the meantime made questionable the desirability of continuing the effort on the present device to the point of making it into a working machine for nuclear physics because it seemed that even under the best conditions its yield would not be competitive. On the other hand, other developments in the field of accelerator theory and design had suggested that the geometry of this machine might furnish conditions under which the total beam intensity could be very much increased over existing levels. One such development involved the injection of an electron beam in neutral equilibrium between space charge and external focal forces (here called a space-charge-limited, or SCL, beam) into the machine aperture in a single turn (2). The small aperture and existing focusing and deflection systems of the original device were adaptable (although not ideally so) to a study of this type of injection. Despite the drawbacks of the existing setup, most of which are associated with a lack of working space and an unfavorable ratio of focusing conductor volume to deflection conductor volume, we felt that we could partly or completely resolve the following questions, answers to which would be of importance for future investigations:

1. Is it possible to inject an external beam into a strong-focused betatron aperture in a single turn?

2. What effects do errors in entrance deflector and main orbit optics have in reducing the contained current below the space charge limit?

3. Can the particle loss mechanisms be understood?

4. Can adequate vacuum techniques be developed to allow the use of oxide emitters and to assure freedom from beam-atmosphere interactions?

1

It can now be reported that the answers to most of these questions are favorable and that a point of diminishing returns in the present experiment, in view of the disadvantages alluded to above, has been reached.

1. It is feasible to inject a beam of at least half the SCL intensity into a small aperture in a single turn. The estimated beam length is consistent with estimates of the quality of the fast entrance deflector and focusing pulses. Various sources for producing pulses of the requisite high level combined with high quality for this application have been developed. These include thyratrons (3) (used in this experiment), spark gaps, and vacuum tubes.

2. It appears that defects in orbit and entrance deflector optics can reduce the contained current to as much as an order of magnitude below the SCL value unless considerable care is exercised. From these results the conclusion is that the intensity suffers by a factor of about 5 from the injector defects and by another factor of about 3 from main orbit defects.

3. Particle losses can be accounted for to an accuracy of about 20 to 30 percent; this corresponds roughly to the experimental accuracy.

4. The vacuum system operates with a sing ⟩ 5-liter Vac-ion pump mounted just above the gun; it involves relatively small bores (~ 1-1/8-inch diameter) and great lengths (8 feet). Despite this the pressure in an ion gage at the point of the system farthest from the pump reads 1×10^{-6} mm under operating conditions, the pressure at the pump being about 3×10^{-7} mm. The pressure in the cold system is a factor of about 10 lower at each position. About two-thirds of the operating pressure results from the bombardment of the Aquadag coating in the upper entrance tube by undeflected beam electrons. These pressures are entirely adequate for operation of oxide-coated emitters and produce negligible gas interaction under present conditions.

DESCRIPTION OF EQUIPMENT

Figure 1 shows several photographic views of the machine, including the flux bars, which provide the betatron acceleration; the injector assembly; the entrance tube; the main orbit field coils; and the focusing system. These are shown schematically in Fig. 2. A block diagram of the electronics is shown in Fig. 3. More or less detailed diagrams of the timing circuits, gun pulse circuit, fast focusing, deflection, and ejector circuits, and the 60-cycle power circuits and monitoring devices are shown in Figs. 4 through 11. Table 1 contains a list of the significant parameters.

The timing sequence can be followed by referring to Figs. 3 and 4. A 60-cps sinusoidal voltage passes through a phase shifter whose purpose is to supply the silicon-controlled rectifier (SCR) switch with a trigger at the correct instant in the cycle to correspond to zero current in the complex ac load presented by the field coils, which are principally inductive, and the lenses, which are principally resistive (Fig. 7). This phase-shifted sine wave is fed to a scale of 10 to reduce the duty cycle of the lenses and thus the heating effect. The SCR switch (Fig. 10) is designed to pass current for approximately one full cycle, the right-hand unit in the figure being triggered by the output of a square-loop transformer at about the instant when the current passes through zero. The useful half-cycle is the second, this one being chosen so that switching transients can have time to decay. Shortly after the beginning of the second half-cycle, at an instant determined by the peaker bias and the field current, the peaker transformer delivers a pulse to the master timer. This pulse is squared and then used to trigger a set of slave timers. These are delay multivibrators followed by 2D21 thyratrons (Fig. 4(b)) and are used to determine the timing of all subsequent events.
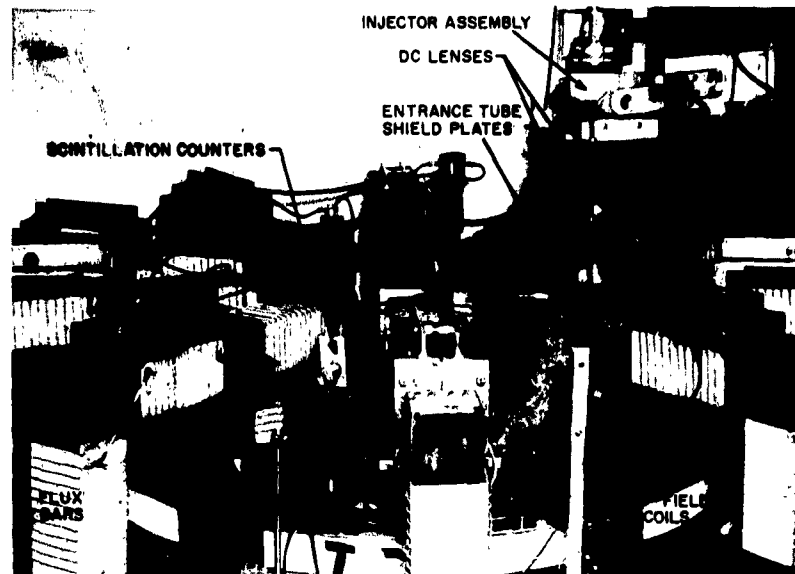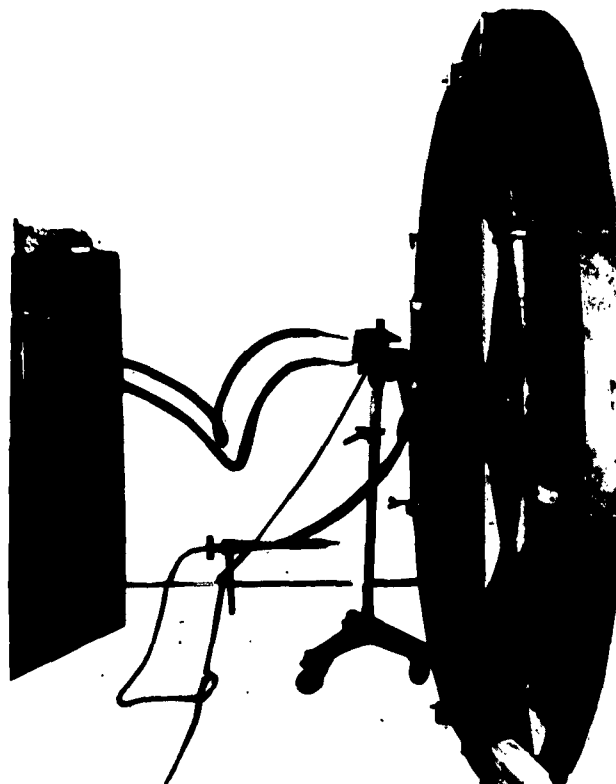
Fig. 1(a) - Five-foot experimental accelerator

Fig. 1(b) - View during assembly of the vacuum
tube, showing tube, showing induction heater in
place for the braze at the Housekeeper seals.
Dry hydrogen is being fed to the interior through
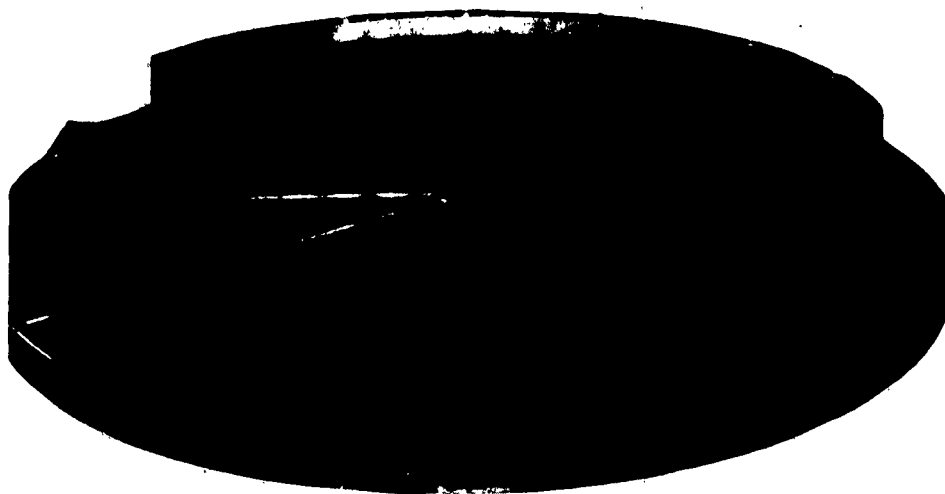the top of the entrance tube.

Fig. 1(c) - View during assembly of the quadrupole focusing
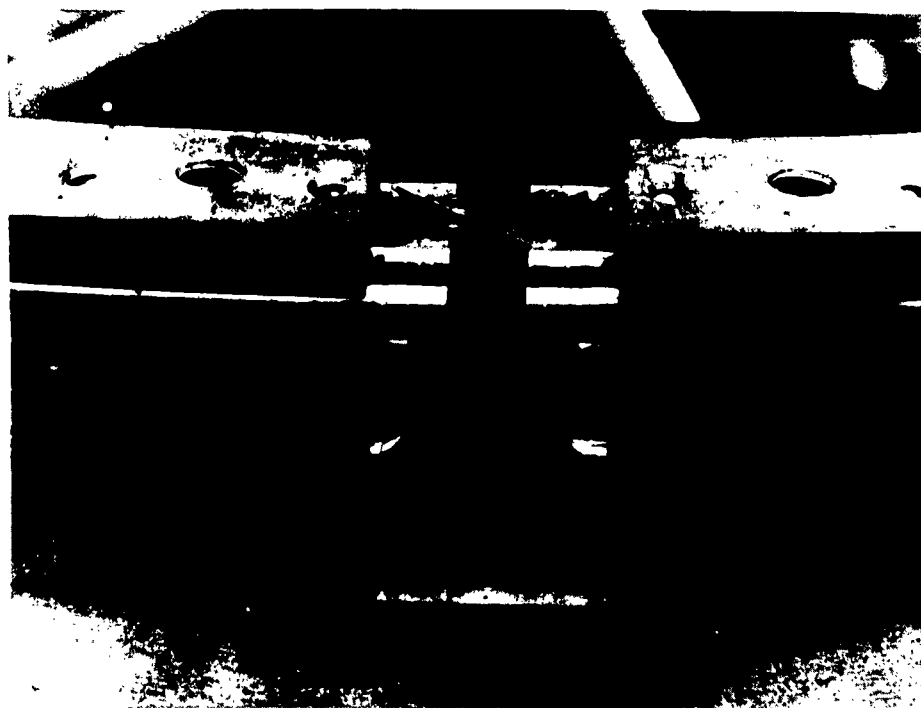system, showing precision jig used to locate the crossovers

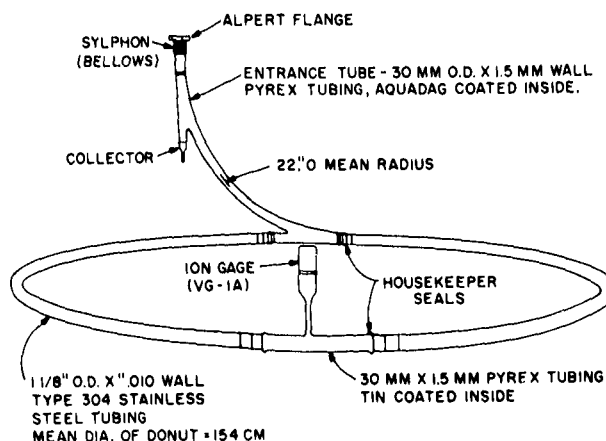Fig. 1(d) - Detail of quadrupole crossover

Fig. 2(a) - Vacuum tube assembly,
viewed from above

One of the slave timers supplies a trigger to the gun pulser, which produces a pulse about 1 μsec long and having the shape of an approximate half sine-wave. During most of this time the gun current passes into a collector (Fig. 2(a)). But at a prescribed instant near the maximum of the gun voltage pulse the fast deflector and focusing conductors are energized for a time roughly equal to two revolution periods of an electron through the machine. The entrance deflection and focusing fields are therefore nearly constant for a time greater than one revolution, thus assuring that there is one full turn of electrons in the machine. The fast deflector is characterized by a dead time, defined as that interval during which there is enough residual field in the fast circuits to destroy the main orbit beam entering from behind but not enough to introduce fresh beam into the tube. We have taken this dead time as the time required for the fast pulse to fall from 98 percent to 2 percent of its maximum value. This amounts to about 20 nsec for these pulsers, that is, about half a turn. We therefore expect to capture about half a turn of the injected beam.

After the disappearance of the fast entrance pulse the behavior of the beam is independent of conditions at the injector. After suffering some real and some apparent losses, the captured beam is retained and accelerated up to a point where it is either ejected by a fast ejector circuit (Fig. 2(f); the power supply for this is substantially the same as that of Fig. 6(a)) or dumped as the result of a shift in operating point caused by electrical misalignment.

The field coils (4) are shown in Figs. 2(a) and 7. These are designed so as to cancel the term in the expansion of the vertical magnetic field on the equatorial plane in the second order of small separation from the center of the aperture. This can be done accurately by means of the linearity adjustment. The gradient (n-value) is set by the gradient adjustment; the measured value is 0.56. These coils have been wound with copper ribbon approximately parallel to the magnetic field to reduce eddy currents.

The lenses (1) are shown in cross section in Fig. 2(c) and in plan (schematically) in Fig. 2(d). The photographs (Figs. 1(c) and 1(d)) show the supporting structure and the jig used in the accurate positioning of the crossovers during assembly. The tolerance aimed for was ±0.002 inch; probably something like three to five times this value was attained. The conductors on each half of the machine were connected to give the relative polarities indicated in Fig. 2(c) (alternating each half-lens). All lens conductors are in series; the polarities are such as to make the two halves of the machine identical. The mode number is adjusted by varying the lens transformer ratio (Fig. 7).
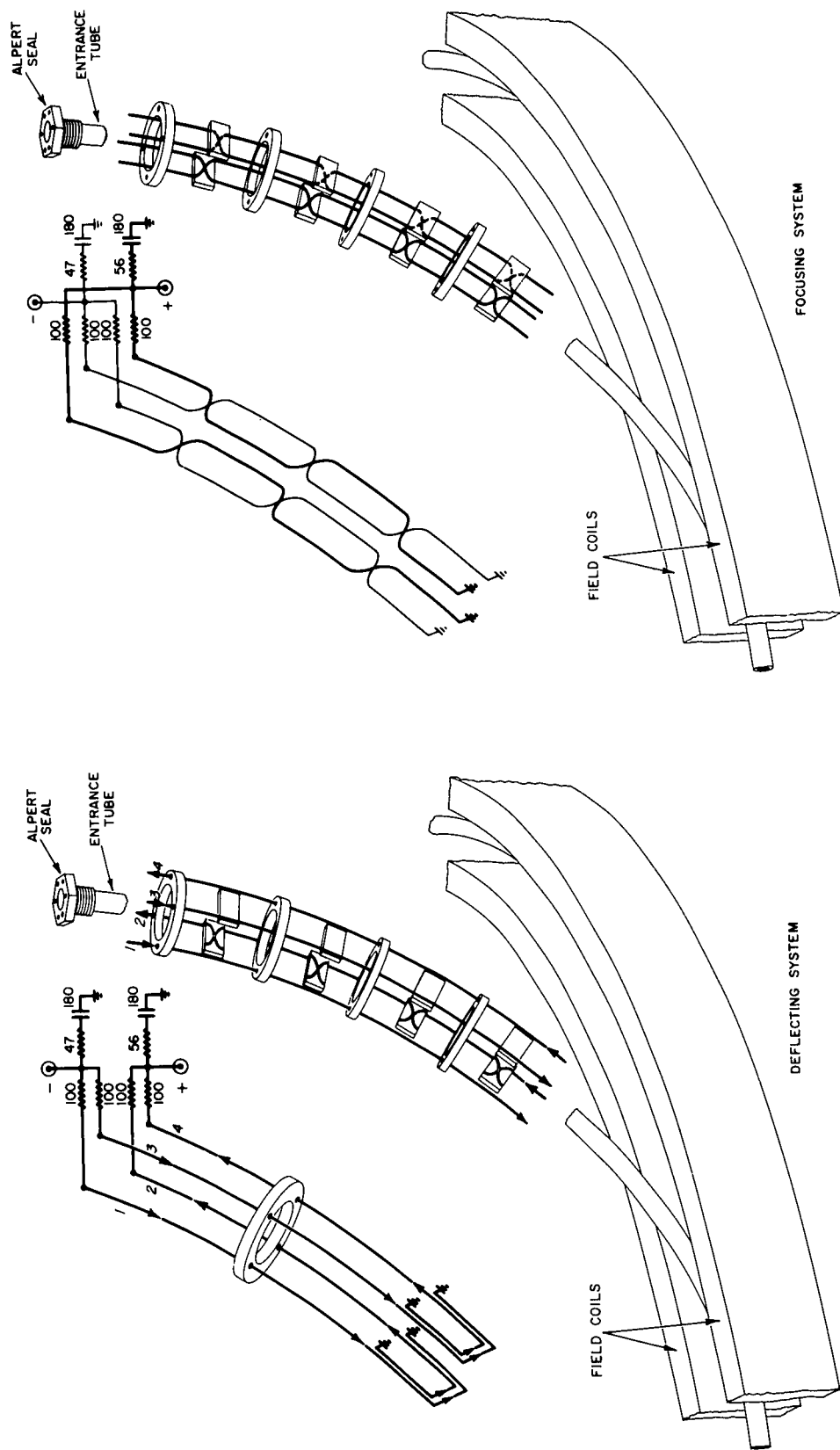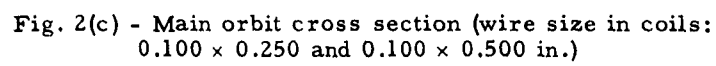
Fig. 2(b) - Schematic of fast deflection conductors on the entrance tube with arrows indicating electron flow (circuits are not shown complete; collector omitted for clarity)

Fig. 2(c) - Main orbit cross section (wire size in coils:
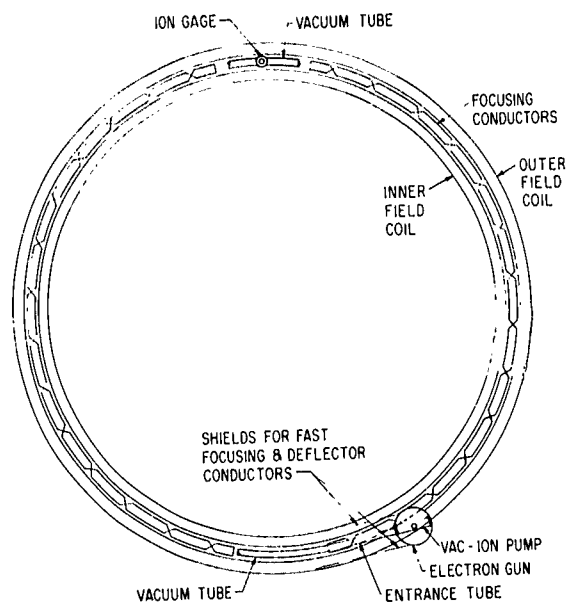0.100 × 0.250 and 0.100 × 0.500 in.)

Fig. 2(d) - Plan view of vacuum tube,
lens, and field coil assembly
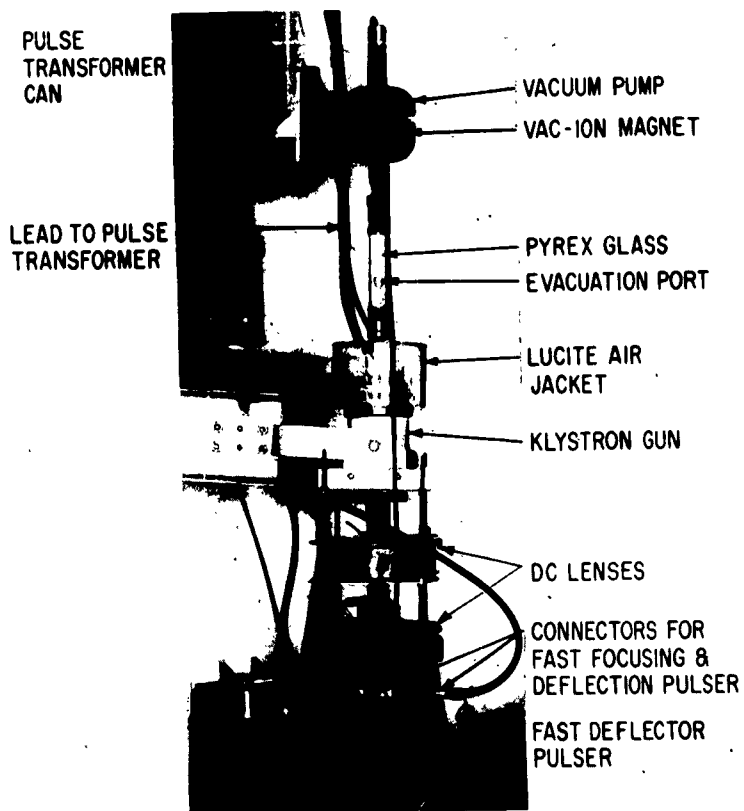
Fig. 2(e) - Electron source and vacuum pump,
viewed from inside the main orbit

Fig. 2(f) - Schematic of assembly in ejector area
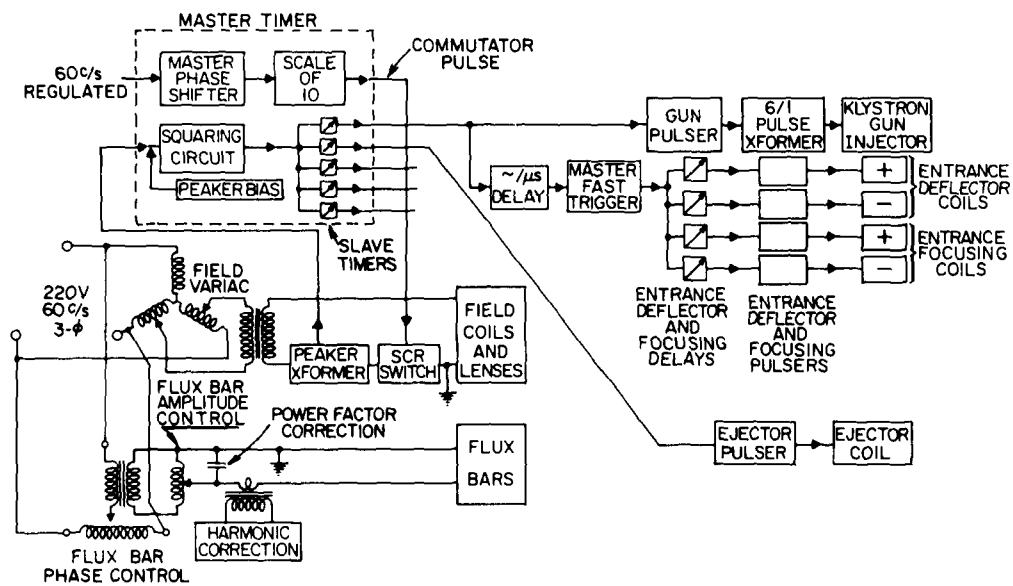
Fig. 3 - The electronics

Fig. 4 - Master timer and typical slave timer

Fig. 5 - Gun pulser

Fig. 6 - Positive and negative deflector pulsers

Fig. 7 - Field coil power circuit

Fig. 8 - Lens current indicator
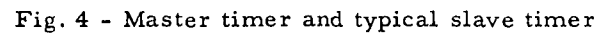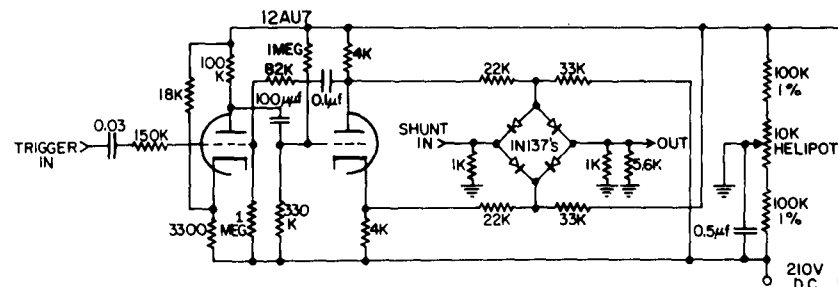
Fig. 9 - Lens-field current comparator

Fig. 10 - Silicon-controlled rectifier switch
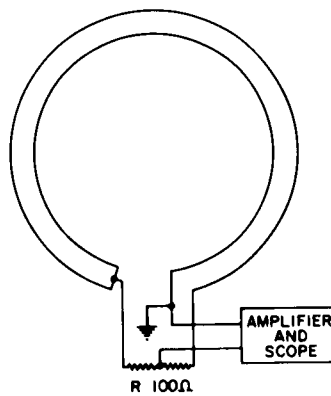
Fig. 11 - Betatron flux condition
monitor

Table 1
Parameters of the Machine
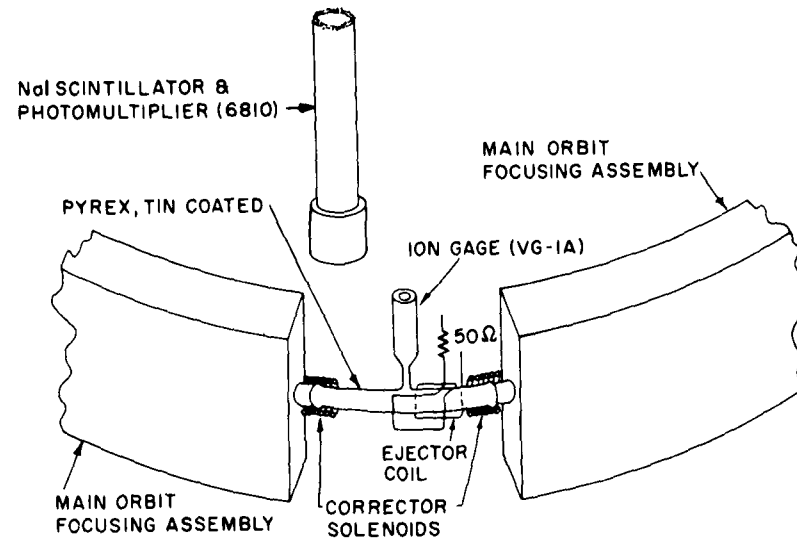
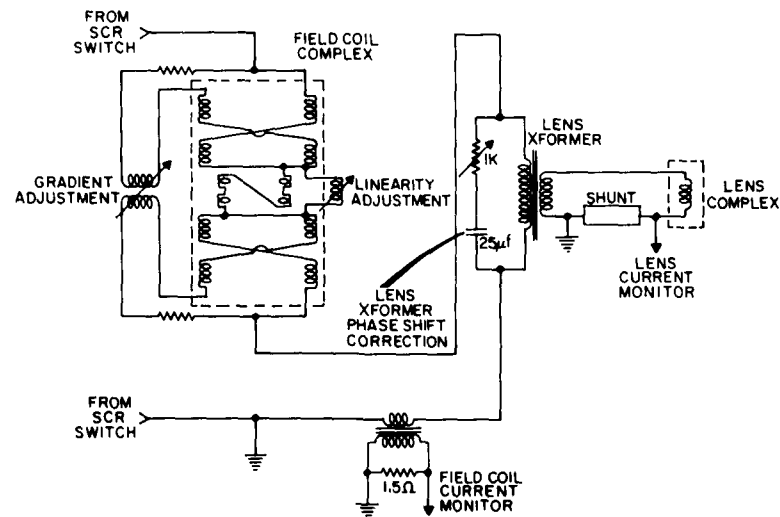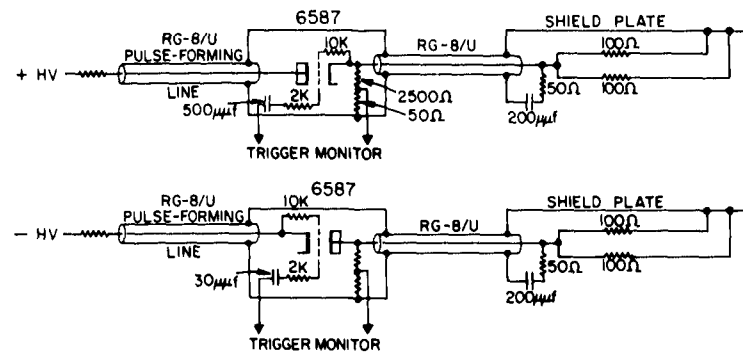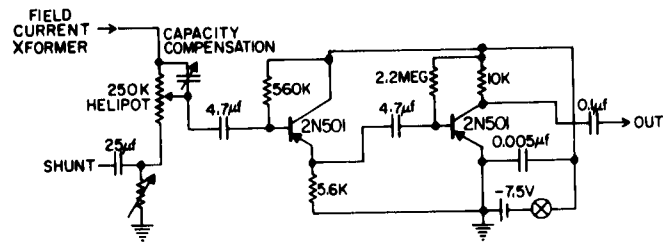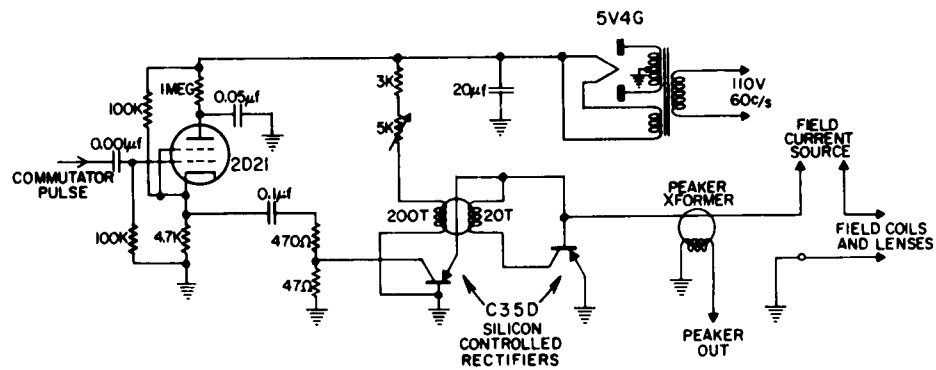|	
Mean Radius:	77 cm
Vacuum tube aperture:	1 inch
Focusing:	45-degree ironless quadrupoles with two unfocused sections each one full lens in length
Number of lenses in circumference:	16 minus 2
Field coils:	Ironless; horizontal aperture for focusing conductors and vacuum tube 1.87 inches, 2.30 gauss/amp
Field coil n-value:	0.56
Betatron wavelength:	Variable; set at approximately 270 cm for work reported here
Electron energy at flux bar saturation:	4 Mev; maximum energy in work reported here held to 2 Mev
Injection system:	Single turn external with pulsed deflection and focusing
Injection energy:	50 kev
Injector pulse length:	1-μsec half sine wave
Fast deflector and focusing pulse length:	80 nsec with 20 nsec fall time
Electron circulation time at injection:	40 nsec
Number of particles captured:	$4 \times 10^9 \pm 25\%$ at 270-cm betatron wavelength.

The entrance deflector and focusing conductors (3) are indicated schematically in Fig. 2(b). Figure 6 shows the electrical circuit of the deflectors. These circuits are completed through the shield plates. The circuits for the focusing wires are the same, except that these operate at higher voltage and, of course, alternate in position as shown in Fig. 2(b). The most severe practical limitation associated with these conductors arises from the situation at the bottom of the entrance tube, where the shield plates, originally substantially separated, must be brought in to allow continuation of the conductors into the region between the field coils. The image currents associated with this reduction in shield clearance are very severe. Their effect can be partly overcome by doubling the number of deflector turns at the lower end of the entrance tube; this can be done by bringing these conductors back from the bottom between the field coils and grounding them at the point where they enter the field coils. The focusing coils, on account of their complicated shape, allow of no such treatment, with the result that the focusing field is badly distorted at the bottom of the entrance tube. There seems to be no way of avoiding this difficulty with the present system. The electrical circuit of Fig. 6 is designed to present a frequency-independent 50-ohm load to the source; this is the purpose of the 50-ohm resistor in series with the 200-$\mu\mu$f condenser at each input point. This has the unfortunate effect of doubling the rise (and fall) times of the current in the conductors, but it was felt to be worth the price in order to remove the undesirable reflections resulting from the mismatch. The fast deflection and focusing pulses are brought into accurate synchronism through the use of a common trigger and passive trimming delays.

The 60-cps power circuit (Figs. 3 and 7) is intended to provide a considerable degree of flexibility in the choice of operating point through the use of a stepwise variable transformer. If this were an ideal transformer with infinite primary inductance, this arrangement would provide exact proportionality between deflection and focusing currents. Because of the finite primary inductance the RC circuit of Fig. 7 is connected across the primary. Correct electrical alignment requires adjustment of this circuit at each step of the transformer. If the alignment is not correct, the operating point will drift and the beam will be dumped at some point before the end of the quarter cycle of field increase. This loss is hard to avoid because the RC compensating circuit corrects the phase error exactly at only one frequency, whereas the transient nature of the pulse involves a frequency spectrum. It is possible to obtain satisfactory beam retention for about 70 percent of the quarter cycle, that is, up to about 85 percent of the peak field. The RC circuit is able to provide a continuously variable operating point if one can tolerate only short-time retention of the beam, and this is useful in studies of the beam over a few turns.

Circuits to monitor the lens current (Fig. 8) and the ratio of lens to field currents (Fig. 9) were found indispensable for proper alignment. The former contains a gating arrangement whereby the shunt signal is presented only during a short (20-μs) pulse. This permits direct comparison with a dc level provided by a calibrating source (100-kilohm precision resistors, Helipot, and regulated 210-volt source) and eliminates phase shift errors introduced by the amplifiers required for the very small shunt signal. Because of grounding difficulties associated with very low level signals it was found necessary to monitor the field coil current with a current transformer, consisting of a Variac core through which the field current was passed and whose primary was loaded with 1.5 ohms. This transformer introduces a quadrature error; therefore a similar error is deliberately introduced by the RC circuit in the shunt arm of the comparator circuit (Fig. 9). The required resistance in this compensating circuit as well as the ratio of sensitivities of the transformer and shunt are found by the use of identical currents. Capacity compensation for various Helipot settings is required for proper balance. A preamplifier is required because of the extremely low level of the null signal. This has an input stage consisting of an emitter-follower to reduce the loading of the high-impedance Helipot circuit.

The betatron flux condition is maintained by adjustment of the flux bar phase and amplitude controls (Fig. 3) and by the injection of phase- and amplitude-controlled third and fifth harmonics produced by locked oscillator-amplifier arrangements; these compensate for nonlinearity in the flux bars. The betatron flux condition is monitored by the use of two conductors, one inside and one outside the orbit (Fig. 11); these were precisely located when the field coils were built. The resistance R is determined by the geometry; its value for these field coils is 1420 ohms. Satisfaction of the betatron flux condition is indicated by a null on the scope. The condition can be satisfied to a fraction of 1 percent over about 90 percent of the quarter cycle of field increase.

The ejector is intended to bring the beam abruptly against the upper wall of the vacuum tube in its neighborhood (Fig. 2(f)). Evidently the possibility of this depends on the energy of the beam, since the ejector current is limited and the conductors are of necessity so placed that there is a considerable cancellation of their fields due to images in the field coil walls. This ejector should be able to produce a deflection of about 15 degrees at the injection energy. This is sufficient to insure that the whole beam strikes the upper glass wall at injection energy and somewhat above. At substantially higher energy the beam strikes the stainless steel part of the donut. Although there is more shielding here, the higher-energy x-rays are produced with greater efficiency and are more penetrating, with the result that the yield at the scintillator, placed about 20 cm above the donut, rises much faster than linearly with energy. The ejector suffers from a dead time corresponding to that of the entrance deflector, but it occurs at the rise of the pulse rather than the fall. During this interval the deflection is sufficient to destroy the beam but inadequate to produce a signal at the counter. The estimated dead time of

the ejector (2 percent to 50 percent) is about 15 to 20 nsec as observed on a scope; the measurement is difficult, and this result is approximate. The detector is a 1-inch square NaI(Tl) crystal, the light from which passes through a Lucite light pipe into a 6810 photo-multiplier. The output is delivered directly to a 50-ohm load. The photomultiplier response is linear up to about 3 volts output. NaI was chosen as a scintillator material because of its high stopping power for radiation of the energy involved and because of its integrating characteristics, which are such that one can obtain an indication of the total radiation emitted during the ejection pulse. Thus, when suitably calibrated, this detector can provide information about the total charge captured which is very hard to obtain in any other way. The large light output and long decay time are also convenient for output measurements.

The electron source (Fig. 2(e)) is a 3K50,000 klystron gun supplied by the Eitel-McCullough Company. This has an emission capability about ten times higher than we required from it. These guns have nickel matrix cathodes and have proved rugged and reliable in this service. The present one has survived at least two exposures to the air after the first activation with no apparent emission loss. The beam from the gun is passed through two lenses with direct current excitation. Their functions are to supply the current density and angular divergence required by the entrance optics and to steer the beam into the entrance tube. Except during the short entrance deflection interval the beam is principally delivered to the collector (Fig. 2(a)), the current from which is monitored as a check on dc lens and gun operation.

The vacuum system consists of the donut (Figs. 1(b) and 2(a)), the entrance tube, the gun, and the Vac-ion pump. The main part of the donut is made of 1-3/16-inch × 0.010-inch-wall stainless steel tubing. The two glass sections (entrance tube and ejector sections) were connected to the stainless steel tubing by special Housekeeper seals having a stainless-to-copper seal at the metal end. This permitted the glass sections to be assembled to both seals, leaving a short stainless tube at each end. The final assembly consisted of induction brazing these protruding ends to the ends of the 0.010-inch-wall half-donut sections (Fig. 1(b)). The stainless steel was nickel-plated before assembly. Dry hydrogen was flowed through the inside and over the outside of the tube during the brazing. It was necessary to limit the wall conductivity to the order of 100 ohms/square in the entrance and ejection regions to allow the fast-rising fields to penetrate. The entrance tube was originally coated with tin deposited from a vapor state. This was found to be adversely affected by electron bombardment, and there was a tendency for thin spots to develop. The tin coating on the entrance tube was therefore replaced by an Aquadag (carbon) surface having about the same resistivity. The coating in the ejector region is tin; here the glass is not exposed to the direct beam from the gun and so is not nearly so severely treated. The Aquadag is not free of difficulties in that it is hard to outgas, but it does appear stable against electron bombardment. The gun is connected to the top of the entrance tube through a sylphon bellows and an Alpert seal. Pumping is accomplished through the Vac-ion pump connected to the cathode end of the gun through a section of Pyrex tubing used as an insulator. It was originally hoped that the whole system, including the gun, could be baked out in a separate oven, sealed off, and put on the machine. For mechanical reasons this turned out to be impossible, so that the system and gun had to be baked out individually and then opened to the air for a short period while the two were joined after the tube was transferred from oven to machine. The final activation of the gun was then accomplished with a trapped mercury pump operating through a port in the glass insulator. Although this had no adverse effect on the gun, the Aquadag coating absorbed a great deal of air. Despite the continued outgassing of this coating, the operation is nevertheless quite satisfactory.

Two other corrections were employed in the machine. The first consisted of a set of small coils capable of producing horizontal and vertical fields at various points along the tube for beam steering. These fields are approximately in phase with the guide field. The

second correction was provided by four small solenoids at the ends of the long quadrupole lens chains; two of these are shown cut away in Fig. 2(f). These solenoids produce a small improvement in yield by partially correcting phase space distortion resulting from the two unfocused regions along the main orbit.

CONSIDERATIONS DETERMINING THE EFFECTIVE APERTURE

The effective aperture of a machine like this will in general be considerably smaller than its physical aperture. This is the result of gas scattering, forced oscillation, free oscillation of the whole beam, and high- and low-frequency ripple. If the first three causes are corrected, one can define a "stop band" as a region of operation in which the effective aperture is zero; if one thinks of it in these terms, it will be clear that operation even near the edge of, although within, a stable cell is a difficult matter because the effective aperture may be so small that only a few particles can get through. The individual quadrupole lenses produce the high-frequency ripple; this does not produce stop bands in normal operation but rather gives rise to a slowly decreasing effective aperture with increasing normalized lens gradient n_o. The unfocused regions, widely separated on the machine, give rise to low-frequency ripple or pulsation of the amplitude and produce stop bands which may be so severe that a useful operating band may be only a few percent wide in n_o.

It is convenient to discuss these ripple losses in terms of phase space distortion. For this purpose we define the phase space coordinates for one transverse degree of freedom as ξ, the corresponding transverse configuration coordinate, and η, the corresponding slope of the trajectory multiplied by the mean betatron radian length. To simplify matters we shall deal only with symmetrical nondeflecting elements. Such elements have the property that the phase space coordinates at a position 2 (output) are related to those at position 1 (input) by the formula

$$\begin{pmatrix} \xi \\ \eta \end{pmatrix}_2 = \begin{pmatrix} \cos\theta & a\sin\theta \\ -\dfrac{1}{a}\sin\theta & \cos\theta \end{pmatrix} \begin{pmatrix} \xi \\ \eta \end{pmatrix}_1$$

in which θ and a are constants related to the element. We refer to θ as the betatron length of the element and to a as the phase space distortion factor. It is easy to verify that the effect of the matrix is first to multiply the η-coordinate by a, then to perform a rotation through the angle θ, and finally to divide the new η-coordinate (subsequent to the rotation) by a. One might be inclined to the view that a must be greater than unity in order to give rise to a particle loss because of the distortion produced in an originally circularly bounded phase space; from the foregoing it is seen that for $\theta = \pi/2$ the transverse coordinate is increased by the factor a, so that beam loss results if $a > 1$ and the beam originally occupies the physical aperture. If $a < 1$, the amplitude should be less after a 90-degree rotation, and there should then be no loss. The fallacy in this argument is that it fails to take account of the particle behavior within the element.

The Cayley-Hamilton theorem or other arguments can be invoked to show that the effect of N identical elements in sequence is merely to multiply the angle of rotation by N; the distortion factor is unchanged. If the elements are symmetrical quadrupole lenses (1/4-lens, 1/2-lens, 1/4-lens) wherein the first 1/4-lens is focusing or defocusing, one finds a to be respectively greater or less than unity. But in the latter case the amplitude has its maximum in the focusing 1/2-lens, where it is nearly as great (for the same initial slope) as in the end-focusing 1/4-lens in the former case. We must conclude that the

high-frequency ripple produces loss if either a or $1/a$ for a single lens exceeds unity. If one denotes by a_+ and a_- the distortion factors corresponding respectively to the first 1/4-lens focusing or defocusing, then the high-frequency retention factor R_H is defined by the formula

$$R_H = a_-/a_+ \ .$$

This is shown in Fig. 12. (For a calculation of the matrix elements see Ref. 1.) In principle this is not exactly the correct retention factor; it should include a factor of the order of unity for such effects as the fact that the maximum high-frequency ripple is confined to the planes of maximum gradient. In practice there are precessive motions of various kinds which make the calculation of this factor difficult and its retention in the formula academic.
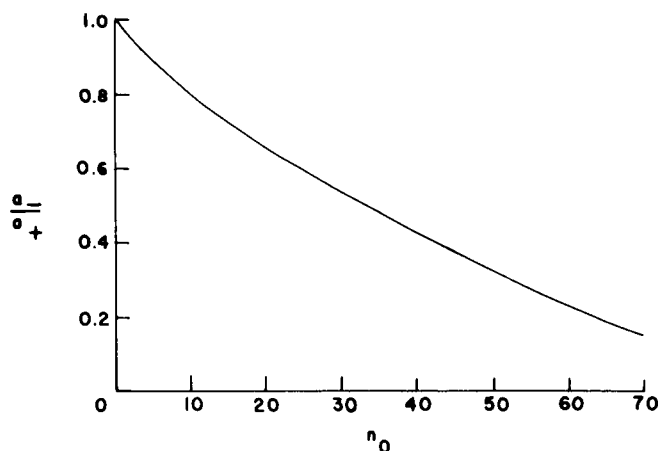

Fig. 12 - High-frequency retention factor

The low-frequency ripple in general contains many betatron wavelengths in one cycle of pulsation. Here one deals with a "compound" element consisting of a sequence of quadrupole lenses with a half-section of unfocused orbit at each end (Fig. 2(d)). Since this compound element has a considerable betatron length, it follows (if the high-frequency effects are not considered) that if an elliptically bounded phase space enters a compound element, it can in general assume any orientation in passing through the element, including, of course, that of the major axis in the amplitude direction. It therefore appears that in consideration of the low-frequency ripple we are also obliged to use the greater of $a_\pm'$ and $1/a_\pm'$ to find the corresponding retention factor, where $a_\pm'$ is the distortion factor for a compound element whose first 1/4-lens is focusing (+) or defocusing (-).

We define, subject to the same stipulation about correction factors near unity as was made above, the low-frequency retention factor

$$R_L = 1/ \ \{a_+'\} \ \{a_-'\}$$

where

$$\{a_\pm'\} = \begin{cases} a_\pm' & \text{if } a_\pm' > 1 \\ 1/a_\pm' & \text{if } a_\pm' < 1 \end{cases}$$

and the total retention factor

$$R_T = R_H R_L.$$

Figure 13 indicates the low-frequency and total retention factors for the present system. Details of the calculations of the matrix elements can be found in Ref. 1. The bars in the figure indicate the total current near the center of each stable cell (without consideration of imperfections) if the tube is initially filled from a source whose current density is inversely proportional to the square of the betatron wavelength. It is suggested that the maximum current should be found near $n_o = 43$, corresponding to a mode number near 2.5. It may be remarked here that the maximum current in practice is found near the center of the next lower cell, at a mode number near 1.5. The discrepancy is probably caused by faulty injector optics, which fail to provide a beam of the required characteristics. The existence of small focal imperfections along the orbit tends to drive the operating point away from the center of the stable cell. From reference to the figure it seems reasonable to conclude that perhaps 30-percent retention is to be expected after allowance for this. It should be emphasized that all these arguments apply to a "temperature-limited" beam, that is, a beam whose current density is determined primarily by its total current and its temperature. A space-charge-limited beam of the current observed in this experiment would be substantially smaller than the physical aperture so that these arguments would not apply. It seems probable that the poor optics at the lower end of the entrance tube give rise to so much beam heating resulting from aberration that it is unreasonable to imagine the beam to be of the SCL type.
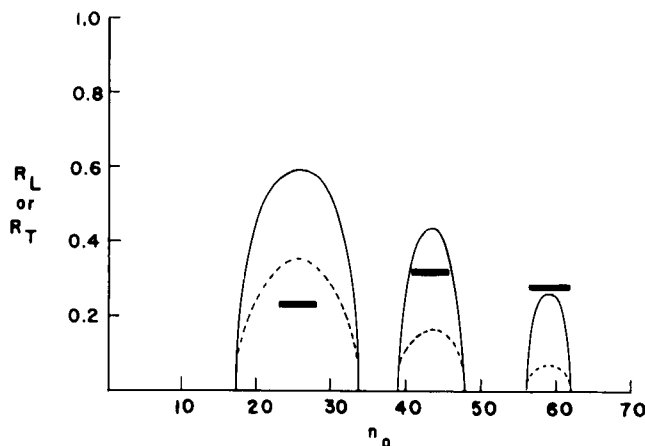

Fig. 13 - Low-frequency retention factor R_L (solid) and total retention factor R_T (dashed). Bars indicate the relative current retained from a perfect source with strength proportional to the inverse square of the betatron wavelength.

It is possible in principle to effect a correction of low-frequency errors produced by an unfocused section bounded by a smooth lens system at each end if a thin lens is placed at each transition to the smooth system. The matrix for a thin lens is

$$(L) = \begin{pmatrix} 1 & 0 \\ -\alpha & 1 \end{pmatrix}$$

where a is the betatron radian length divided by the lens focal length. The matrix for the unfocused section is

$$(U) = \begin{pmatrix} 1 & k \\ 0 & 1 \end{pmatrix}$$

where k is the length of the section divided by the betatron radian length. Therefore the matrix for the whole corrected section is

$$(L)\ (U)\ (L) = \begin{pmatrix} 1 - ak & k \\ a^2 k - 2a & 1 - ak \end{pmatrix}.$$

This corresponds to a pure rotation ($a = 1$) if $k = 2a/(1 + a^2)$. Complete correction is therefore not possible if $k > 1$.

To find the effect of such a correction on the actual quadrupole system, the matrix

$$\begin{pmatrix} 1/2 \text{ unfocused} \\ \text{section} \end{pmatrix} \begin{pmatrix} \text{thin} \\ \text{lens} \end{pmatrix} \begin{pmatrix} 7 \text{ quadrupole} \\ \text{lenses} \end{pmatrix} \begin{pmatrix} \text{thin} \\ \text{lens} \end{pmatrix} \begin{pmatrix} 1/2 \text{ unfocused} \\ \text{section} \end{pmatrix}$$

was calculated for various thin lens strengths. The theoretical results indicate an improvement of about 20 percent in the yield with $a = 0.25$ and the mode number $M \sim 1.5$; this value of a gives about the best correction in this case. Doubtless more sophisticated methods of phase space correction could have been attempted, but in view of the limited space this was probably about the best that could be done. With the present correction applied we should look for a retention of about 36 percent of the injected beam in the absence of other errors.

BEAM DETECTION AND CURRENT MEASUREMENT

One of the most difficult problems in this experiment is the assessment of the charge contained and maintained in the ring. The limited working space between vacuum tube and field coils leaves very little room for a current transformer. Any such device is, because of the geometry, forced to have a short integration time. Therefore the beam has to be destroyed quickly if a useful signal is to result. The pulse used to destroy the beam generally involves currents very much larger than the beam current, a circumstance leading to a very poor signal-to-noise ratio. So, although some measurements along this line were attempted, they were quite unsatisfactory.

The method finally used involves an integrating detector in conjunction with a fast ejector. The detector was calibrated by observing the response to a known charge striking a target of (ideally) the same material and thickness and at the same energy as under measurement conditions. The vacuum tube is so constructed that the entrance tube section can be electrically isolated from the rest of the donut near the two Housekeeper seals at each end. By bridging the gap (which is very narrow, merely a scribe line on the glass coating) with an electrometer it is possible to find the average current delivered from the entrance tube to the donut; since the duty cycle is accurately known, the peak current delivered during the pulse is known as well. The entering beam can be sharply deflected upward against the entrance tube wall with an external magnet placed near the bottom of

the entrance tube with the scintillator located at a substantial distance from the target area on the glass. The signal delivered by the scintillator is then proportional to the known peak current and the known entrance deflector pulse length. The assumptions on which the accuracy of this calibration rests are the identity of the targets at the bottom of the entrance tube and at the ejector position, the indication by the scintillator of the same total charge as given by the electrometer, and the identity of electron energy at calibration and measurement. A measurement in reasonable agreement with theory indicates that the glass wall forming the target is about one-third of an absorption length in thickness at injection energy, so that an estimated tolerance of ±10 percent in wall thickness gives about ±3 percent error from this source. Comparison of the scintillator response at the bottom of the entrance tube with and without the deflecting magnet indicates that about 14 percent of the beam registered on the scintillator does not belong to the deflected component. Because the energy gain at injection energy is only about 250 ev/μsec, one requires about 20 μsec for a 10-percent energy increase. Therefore over short periods which are nevertheless sufficient to include many turns one can assume constancy of energy. With the combined uncertainties it is probably not reasonable to consider the accuracy to be better than about ±20 percent.

Since the beam initially fills only part of the tube longitudinally due to the dead time of the entrance deflector, one would expect that as a result of small energy differences among the beam particles there would be a slow lengthwise beam spread which would ultimately make the beam close on itself. Therefore even if there were no actual particle losses during this spreading period, one would still expect a diminution in peak intensity. If the ejector had zero dead time, this diminution would be of no concern, since the scintillator reads the total charge impinging on the target area. Because of the dead time, however, there is a finite detector integration period determined by the overlap of the beam transit past the ejector and the effective ejection interval (circulation time minus dead time); under circumstances of no overlap the scintillator will show no signal even though there may be a substantial beam in the tube.

To simplify the discussion suppose the longitudinal density function (Fig. 14) to be centered about $\theta = 0$, so that we have a rotating coordinate system centered azimuthally on the beam center, and to be square in θ with a width θ_1. We can by hypothesis assume that the ejector function (probability that a particle passing the ejector will register at the detector by means of its radiation) is of square form, unit amplitude, width θ_0, and centered at θ_2. It will be seen that the ejector dead time corresponds to the "dead angle" $2\pi - \theta_0$ and that θ_2 is determined by the ejector delay. Suppose the whole charge to be constant so that the height h of the density function satisfies the requirement $h\theta_1 = 1$ as θ_1 increases with longitudinal spreading of the beam. We denote by s the product of the density and gate functions integrated over a cycle. Then we can distinguish four cases.
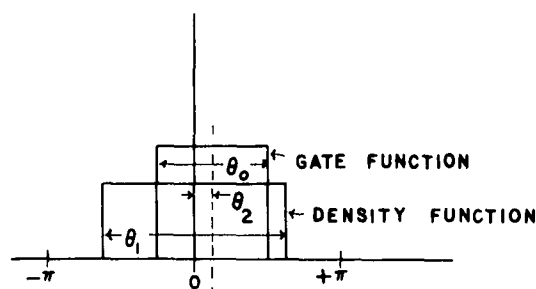

Fig. 14 - Hypothetical beam and gate distribution functions

(1) $\theta_o > \theta_1$, $\theta_o + \theta_1 < 2\pi$

$$s = \begin{cases} 1, & 0 < |\theta_2| < (\theta_o - \theta_1)/2 \\ 0, & (\theta_o + \theta_1)/2 < |\theta_2| < \pi \\ \text{linear transition,} & (\theta_o - \theta_1)/2 < |\theta_2| < (\theta_o + \theta_1)/2 \end{cases}$$

(2) $\theta_o > \theta_1$, $\theta_o + \theta_1 > 2\pi$

$$s = \begin{cases} 1, & 0 < |\theta_2| < (\theta_o - \theta_1)/2 \\ (\theta_o + \theta_1 - 2\pi)/\theta_1, & |\theta_2| = \pi \\ \text{linear transition,} & (\theta_o - \theta_1)/2 < |\theta_2| < \pi \end{cases}$$

(3) $\theta_o < \theta_1$, $\theta_o + \theta_1 < 2\pi$

$$s = \begin{cases} \theta_o/\theta_1, & 0 < |\theta_2| < (\theta_1 - \theta_o)/2 \\ 0, & (\theta_1 + \theta_o)/2 < |\theta_2| < \pi \\ \text{linear transition,} & (\theta_o - \theta_1)/2 < |\theta_2| < (\theta_o + \theta_1)/2 \end{cases}$$

(4) $\theta_o < \theta_1$, $\theta_o + \theta_1 > 2\pi$

$$s = \begin{cases} \theta_o/\theta_1, & 0 < |\theta_2| < (\theta_1 - \theta_o)/2 \\ (\theta_o + \theta_1 - 2\pi)/\theta_1, & |\theta_2| = \pi \\ \text{linear transition,} & (\theta_1 - \theta_o)/2 < |\theta_2| < \pi . \end{cases}$$

These results can be summarized as follows:

$$s_{max} = \begin{cases} 1, & \theta_1 < \theta_o \\ \theta_o/\theta_1, & 2\pi > \theta_1 > \theta_o \\ \theta_o/2\pi, & \theta_1 > 2\pi \end{cases} \quad , \qquad s_{min} = \begin{cases} 0, & \theta_o + \theta_1 < 2\pi \\ (\theta_o + \theta_1 - 2\pi)/\theta_1, & \theta_o + \theta_1 > 2\pi \end{cases}$$

where s_{max} and s_{min} indicate the maximum and minimum of s over $|\theta_2|$; the last relation in s_{max} implies that no further nonuniformities in density exist after the beam has closed on itself. This cannot of course be exactly true, but the approximation suffices for the present purpose. Figure 15 shows these functions for various values of θ_o. It is seen that there is a drop in s_{max} corresponding to an increase in θ_1, which in this case represents an apparent loss rather than a real one. If a real loss were present in addition, the functions s_{max} and s_{min} would have to be multiplied by the proper attenuation function.

Another fairly obvious apparent loss occurs in estimating the captured current as compared with that delivered to the ejector after a half turn. In the latter case the effective integration time is the shorter of the total ejector pulse length and the entrance deflector pulse length (at best overlap); the electron circulation time is not involved. In the former case, on the other hand, the effective integration time at best overlap is, as we have seen, the shorter of $(\theta_1/2\pi)t_o$ and $(\theta_o/2\pi)t_o$, where t_o is the circulation time. Since the entrance deflector and ejector pulses are deliberately made considerably more than one turn in length, while because of the entrance deflector dead time the captured beam is initially considerably less than one turn in length, this apparent loss may be quite substantial.
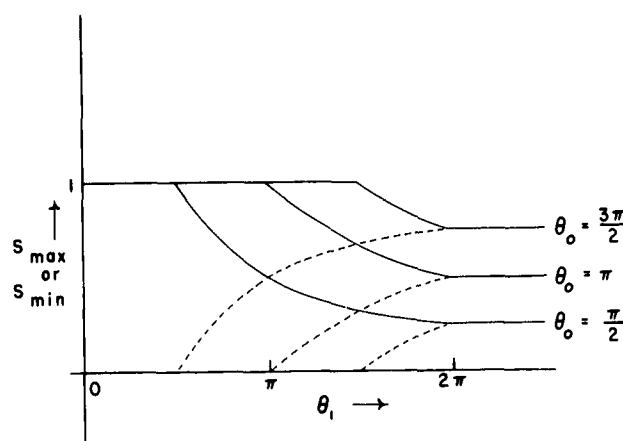
Fig. 15 - Maximum (solid) and minimum (dashed) response of an integrating detector for various values of gate angle (θ_o) and beam angle (θ_1)

EXPERIMENTAL RESULTS

As indicated above, the best current in the machine was found in the cell centered about $M = 1.5$. This is not in agreement with the theoretical prediction as to the best operating point, and one should probably blame the source for this difficulty. The determination of the mode number at which the experiments were conducted was carried out by means of the circuits of Figs. 8 and 9, together with previous theoretical results (1). The formula $n_o = |(\Delta I/\Delta R)|(R/H_g)$, where ΔR is the separation in a 45-degree plane of the measurement point from the equilibrium orbit, $|\Delta H$ is the lens field at the measurement point, R is the equilibrium orbit radius, and H_g is the guide field, can be applied to this lens geometry to give the formula

$$n_o = (16 \; i_{lens}/a^2) \; (R/H_g) \; (\cos 16.8°) \; Q$$

where i_{lens} is the current in one of the eight lens conductors (Fig. 2(c)), 2a is the separation between diagonally opposite conductors, 16.8 degrees is the angular separation between adjoining conductors (see Ref. 4 for a derivation of this correction term), and Q is an end correction due to the lens crossovers. This has been estimated to be about 0.89 from the measured lens field shape. The guide field is determined in terms of the field coil current by the gauss/ampere figure for the coils. When the numbers are put in, one has

$$n_o = 7.6 \; i_{lens}/i_{field} \; .$$

The measurement gives $n_o = 38$. The guide field can also be estimated from the known injection energy, which gives $n_o = 31$. This agreement is not particularly good, although quite a few separate measurements are involved in each determination; thus the ratio method involves a previous calibration of shunt sensitivity vs current transformer sensitivity and the gauss/ampere figure, while the current method entails a knowledge of the injection energy. In view of this disagreement, about the best one can do is to conclude from Fig. 13 that the operating point is on the upper portion of the lowest stable cell shown and thus that $M = 1.8$ is probably rather close to the correct value.

A calculation based on the formula from Ref. 2 for the space-charge-limited current density $j = (8500/\pi) \, (\beta \, \gamma)^3 \, \varkappa_\beta^{-2}$ (j = current density in amps/cm², $\beta \, \gamma$ = electron momentum in relativistic units, $\varkappa_\beta$ = betatron radian length) indicates that the total space-charge-limited current in a cylindrical beam 1 cm in radius is 0.4 amp at 50 kev, $M = 1.8$, $R = 77$ cm. The electrometer measurement of the total current delivered to the donut under optimum conditions indicated a peak current of 210 ma, about half the SCL value. This loss is almost certainly due to the entrance optics, since we have had no difficulty in deflecting an SCL beam through a mockup of this entrance tube under substantially dc conditions (5). When the scintillator was placed above the glass at the bottom of the entrance tube and this entering beam was deflected upward by a magnet, account being taken of the 10 to 15 percent reading produced by stray electrons at the bottom of the entrance tube, the detector reciprocal sensitivity at 80-nsec integration time, 1950 volts on the photomultiplier, at 19 cm from a 1.5-mm-thick Pyrex glass target was found to be 70 ma/v (beam milliamperes per volt delivered from the photomultiplier). For this measurement it was necessary to provide shielding in the neighborhood of the collector (Fig. 2(a)) to avoid saturating the photomultiplier with radiation from the undeflected beam. The detector was then moved to the position shown in Fig. 2(f), also 19 cm from the target area. Using the calibration previously obtained showed that the current passing through the first 180 degrees of the tube was 70 ma. Since only half the tube is involved, none of this loss can be ascribed to low-frequency pulsations. Figure 12 shows that one should expect a high-frequency loss of about 50 percent if the entrance to the main orbit tube is illuminated with a circularly bounded phase space corresponding to the physical aperture. (If entrance and main orbit optics were identical, most of this loss could be eliminated, but such an ideal assumption is not tenable here.) It is likely that the remaining loss of about 17 percent of the entering beam results from uncorrectable errors at the lower end of the entrance tube. The beam captured at the second turn has an indicated intensity of 28 ma based on an integration time of 20 nsec, or about half a turn. According to the estimate on p. 19 of the effect of thin-lens phase space correction (improvement of a factor of 1.2 in the retention) and an estimated 50 percent retention based on the R_L curve of Fig. 13 at $n_0 = 31$, the retained current should have been 42 ma if a current of 70 ma is injected after high-frequency losses have been accounted for. Actually if precessive motions are present, only part of the high-frequency loss occurs in the first 180 degrees of the tube. In any case we have failed to give an explicit accounting for 17 percent of the injected beam of 210 ma and for 20 percent of the remaining beam of 70 ma at 180 degrees. Of course, since the mode number is not accurately known, there is a good deal of uncertainty about the latter loss, and it must be considered within the possible error under present experimental conditions.

Scintillator responses for short and intermediate times are given in Figs. 16 and 17. The plot of maximum and minimum scintillator response shown in Fig. 17 is of similar form to the theoretical curve of Fig. 15 for $\theta_0 = \pi$. That there are no real losses in the intermediate time region is suggested by the constant height of the locus of maxima up to about 2 μsec. No modulation of intensity with ejector delay is perceptible after about 8 μsec, while the disappearance of the modulation coincides with the cessation of the slow diminution of the maxima. It was this coincidence which in fact first suggested the significance of longitudinal beam spreading. Without trying to draw accurate conclusions from Fig. 17, one is nevertheless justified in the notion that the ejector gate and the initial beam are both about a half-turn in length. Accurate conclusions are not possible since the hypothetical gate and beam shapes used to develop the curves of Fig. 15 are certainly only qualitative approximations. It is of interest to estimate the electron energy differences required to give rise to the observed spreading time of about 8 μsec. These are of the order of an electron-volt and can thus be regarded as essentially thermal.

There is no diminution in the pulse height after the beam has closed on itself. The pulse height remains nearly constant out to about 20 μsec when examined on a short time scale. It is, in fact, slowly increasing; if the time base is taken as 2000 μsec rather than 20 μsec, this increase is very marked (Fig. 18). It is much greater than can be accounted for on the grounds of increased x-ray energy until consideration is given to the increased
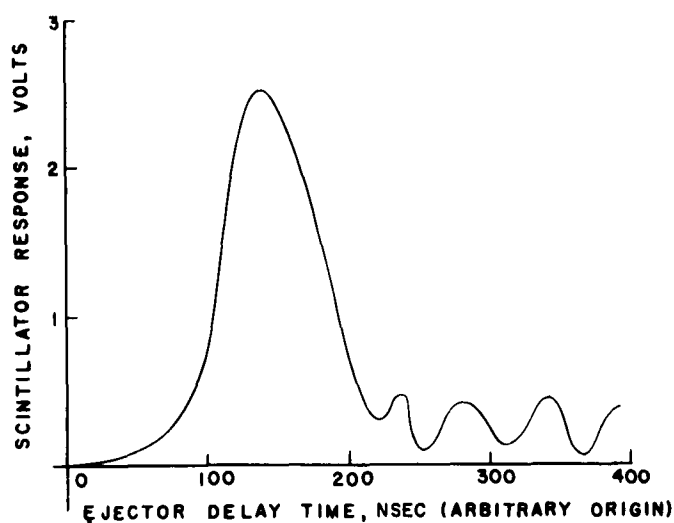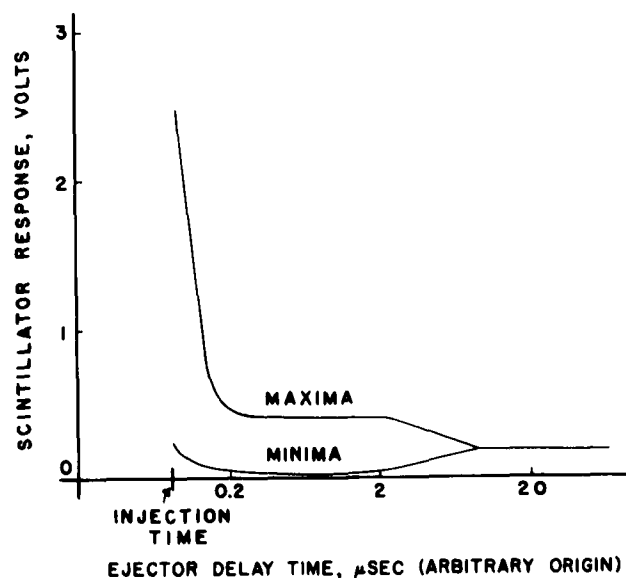
Fig. 16 - Observed short-term beam behavior

Fig. 17 - Observed intermediate beam behavior

penetrating power and efficiency in the production of the radiation. One must conclude that up to about 800 μsec the beam is still soft enough that all its radiation can be seen by the scintillator in the position of Fig. 2(f). After this time the target area moves farther and farther from the detector because of the fixed amplitude of the ejector pulse, while, however, the intensity and penetrating power of the radiation continue to increase. These two effects tend to offset each other, as indicated by the plateau in Fig. 18. That this is not a real effect resulting from loss in beam intensity can be shown by moving the detector closer to the ejector coil; this causes the plateau to set in at earlier ejection times. The drop in intensity at about 2500 μsec represents dumping of the beam resulting from misalignment. The scintillator has a strong response in this range of times with the ejector off.
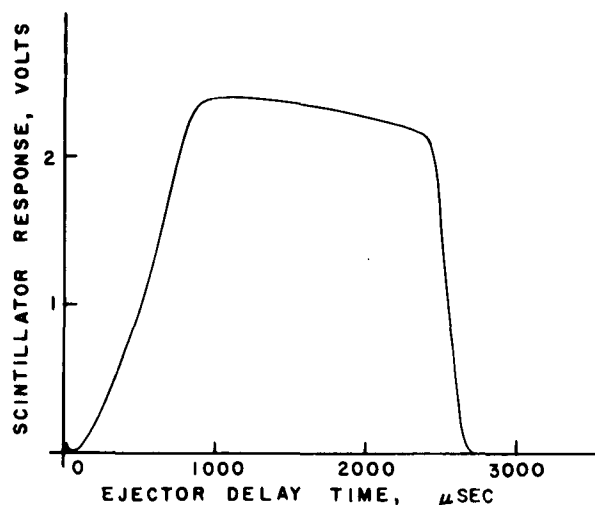
Fig. 18 - Observed long-term behavior

One must regard the evidence that there are no long-term beam losses as strong, though presumptive. The smooth behavior of the curve of Fig. 18 combined with the absence of intermediate loss furnishes part of the evidence. Another part is furnished by the response of a battery of scintillators which were used to survey the vacuum tube during operation; these showed no response in the long-time region up to the dumping period near 2500 μsec. It would be a very good thing if we could have a direct current measurement to provide positive confirmation of the present judgment that there are no long-time losses; meanwhile this statement has to be considered probable rather than certain.

CONCLUDING DISCUSSION

It is with some nostalgia that this project is finally set aside, and it is perhaps appropriate to enumerate here some of the more significant things that have been learned from it, not only during the period covered by this report, but during its earlier existence as well.

1. The inherently small aperture required by the constant-radius accelerators (betatrons and synchrotrons) led M.H. Johnson and the author to consider the possibility of carrying the design to the extreme of a cross-sectional diameter independent of the orbit diameter. This represented a radical departure from existing accelerator design at the time (1948); events have shown the concept to be sound.

2. The necessity of getting the beam through the resulting long, thin pipe was the mother of the invention of the strong-focusing principle (betatron wavelength independent of machine radius), although we found out later that it had been enunciated several years earlier by Wideroe. We demonstrated this principle in a straight tube of length equal to about one-third the machine circumference and having the same bore in December 1951. The first evidence of a captured beam was obtained in October 1952, demonstrating the applicability of the principle in an accelerator geometry.

3. What has to be regarded as a negative result, with, nevertheless, some value in accelerator design if only for that reason, proceeded from the work of the ensuing years. It was realized that the solenoid lenses used in the first experiments could not accommodate the high currents required to maintain a constant betatron wavelength, and a great many attempts were made to drive the machine operating point through the resulting

imperfection resonances, using various kinds of correction circuits together with rapid resonance traversal. It was possible to cross the half-integer resonances with relatively little loss, but the integer resonances proved to be insuperable obstacles.

4. Quadrupole lenses, invented independently by Christofilos and Courant, Livingston, and Snyder, appeared better adapted to the geometry of our machine than did the solenoids used in the first experiments, since they require less magnetic stored energy and consequently less current for the same focal strength. The specific disadvantages of quadrupole lenses are covered in the present report. Despite the disadvantages these lenses were incorporated in the machine, and they have performed adequately. The contained current is a factor of about 15 below the space-charge-limited value for a beam filling the tube to its maximum inner diameter. About half this factor is accounted for in the beam actually delivered to the main orbit. Of the delivered beam about 50 percent is lost by high-frequency ripple in the first half-turn and 17 percent is lost in the same region due to other, unknown, causes. Of the remaining 33 percent of the injected beam about 40 percent is lost by low-frequency ripple (almost all of this loss being in the second turn), 20 percent cannot be accounted for, and the remaining 40 percent survives. There appear to be no losses after the second turn.

The last point gives a broad accounting for the entering electrons. We have now to attempt to profit from this lesson for future work. Probably the worst single loss occurs in the entrance deflector, leaving a beam with only about half the SCL current. This is the result of unsatisfactory injector optics; this defect also leaves the beam with a free oscillation which doubtless causes further losses. Clearly the improvement of the injector optics is one of the most important steps to be taken in the design of future machines after this general pattern. The other severe losses are ripple losses. These are reduced by increasing the effective aperture, this in turn can be effected by either increasing the physical aperture or reducing the phase space distortion or by both. In the latter connection the solenoid lenses, which are free from cylindrical astigmatism, seem to offer a definite advantage. In using these in a practical design one should put most of the bulk into the lenses rather than the deflecting conductors if problems of heat dissipation and resonance traversals are to be minimized.

ACKNOWLEDGMENTS

REFERENCES

1. de Packh, D.C., "Fundamental Considerations in the Lens System of the NRL Experimental High-Current Betatron-Synchrotron," NRL Quarterly on Nuclear Science and Technology, p. 31, July 1958

2. dePackh, D., Roess, H.R., and Godlove, T.F., "An External Injector for the NRL Synchrotron," NRL Quarterly on Nuclear Science and Technology, p. 37, July 1956

3. Godlove, T.F., Kaiser, H.F., Roess, H.R., and Mayes, W., "Design and Construction of an External Injector for the NRL Synchrotron," NRL Quarterly on Nuclear Science and Technology, p. 13, Oct. 1958

4. Godlove, T.F., and dePackh, D.C., "Synchrotron Field Coil Design," NRL Quarterly on Nuclear Science and Technology, p. 13 Oct. 1958

5. Roess, H.R., Laboratory notes, unpublished